Impact of harsh grinding on the structure and color of LiCoPO4 and LiNiPO4 pigments

Hugo Ravet, Nicolas Penin, Anthony Chiron, Cyril Brochon, Fabrice Brunel, Mathieu Duttine, Elodie Bourgeat-Lami, Manuel Gaudon

From the few main colors to their spectra: discussion on robustness or mutability of a material's color.

Hugo Ravet, Nicolas Penin, Anthony Chiron, Manuel Gaudon*

CNRS, Univ. Bordeaux, Bordeaux INP, ICMCB, UMR 5026, F-33600 Pessac, France

* Corresponding author: manuel.gaudon@u-bordeaux.fr, Orcid : 0000-0002-6918-2004

KEYWORDS: Color; CMJ; RVB; Metamerism; Chromogenism

Abstract

The present work intends to bring a new approach for the creation of target colorations in pigment research and development. Rather than proposing a "chemist's" approach, i.e. based on knowledge of the accessible energy levels of the electrons in matter whose transfer will produce absorption phenomena, we propose here, "without any compositional guide", to establish the spectra corresponding to the 6 main colors (red-green-blue-cyan-magenta-yellow): the created spectra for the modelling are created without trying to correspond to any specific composition. Hence, we propose herein a "process" which can be directly transferred to experimental spectra associated to experimental compounds, whatever their nature: organic or inorganic, metallic, semi-conducting or insulating, etc. Since "out of all compositional guide" does not mean "unrealistic", we have first shown that inorganic pigments, which are made up of absorption phenomena associated with the three main types of electronic transfer, can be robustly simulated in absorbance space by a linear combination of Gaussian functions.

Briefly, this work led us to show several interesting conclusions in successive stages:

- A single phenomenon can already create yellow, magenta and blue colors with very good agreement,
- All colors can be created with two-Gaussian spectra,
- Very different spectra can lead to exactly the same coloration (metamerism, which is already largely documented in literature). We showed that these "metameric" spectra then have properties of robustness (maintenance of coloration) with respect to a change of the illuminant or a shift in the energy position of the absorption bands, which can be highly variable. Some colorations are intrinsically more robust than others to these environmental changes.

1. Introduction

The two main reference books focusing their attention on the ways in which colour can be produced in materials are probably the K. Nassau "The Physics and Chemistry of Color" [1] and the R.J. Tilley "Colour and the Optical Properties of Materials" [2]. Considering both the chemical and the physical origins of the coloration of materials, K. Nassau detailed 15 causes of color. For R.D. Tilley, 9 classes of phenomena can be distinguished. In this article, the choice is made to only focus on chemical coloration whose origin is always an electronic transfer (from the inelastic collision of photons within the matter). Chemical colors are the working object of dyes and pigments manufacturers or researchers, and in a way, the kick-off of the occidental industrial chemistry could be marked by the mauveine discovery (synthetic purple dye) by W.H. Perkin [3]. As claimed by the famous citation of Leigh Hunt: "colors are the smiles of Nature" [4], limiting to chemical origin of materials coloration, we would say: "the electrons' travels inside the matter produced by light irradiation let traces, whose colour makes the beauty".

In this article we propose a simplified approach to relating chemical coloration based on electron transfer to color. This is achieved using a simple fitting relation, first with three basis shapes for absorption spectra and using finally only Gaussian functions. Secondly, this simplification allows easy modelling of various colours with Gaussian-based spectra and we will demonstrate than 2-Gaussian spectra are enough to produce the six "main" colours, i.e. the three primary colours in additive and subtractive "color models": Red, Green, Blue, Cyan, Magenta and Yellow,

respectively [5]. These 2-Gaussian based spectra are textbook cases to illustrate that a surjective function (onto function [6]) is linking a "single" color and various associated spectra (third part). Hence, it will be shown in a last part that from this "*surjection*" a color can be robust or on the contrary mutable *versus* energy shift of the absorbance phenomena which can be linked to chemical modification, temperature impact (as in thermochromic effect [7-11]) or pressure impact (as in piezochromic effect [12-14]). Also, from this "*surjection*", leading to the chromatic adaptation transform by the human brain [15], a color can be in a same way robust or on the contrary mutable *versus* illuminant changes ("metamerism" [16-18]), but this time, with interesting redundancies of the robustness or the mutable behaviour depending on the color itself.

2. Results and discussion

2.1. Prerequisites for color modelling

Briefly, the color of solid matter can be classified in 4 main origins: physical subtractive systems, chemical subtractive systems, physical emissive systems and chemical emissive systems [19]. The non-luminescent pigments or dyes, on which we limit our discussion, are among the chemical non-emissive systems. Indeed, it can be distinguished emissive systems, which radiate visible wavelengths, from subtractive systems, which deviate and/or absorb a part of the wavelength issued from a source (an emissive system). In the first cases: emissive systems, the origin can be a physical parameter as temperature (incandescence/black body radiation) or from electron transfer created, for illustration, from light/matter interactions (photoluminescence). In second cases also, the light matter/interaction can be qualified from two case categories. (i) From "a physical interaction" in which only the description of light as an electromagnetic wave is sufficient (with an elastic deviation of the light by the matter whatever the phenomenon is interference, diffraction, scattering, refraction, etc.). (ii) From a "chemical interaction" involves electron transfers (associated to an absorption phenomenon) from photon "impacting" the matter (corpuscular light description). Importantly, the 3 main (primary) colors are red/green/blue in emissive (additive) "color model" since an elementary mixing of these three primary colors allow the obtaining of all colorations (combining red, green and blue gives white). In subtractive "color model", the three primary colors are yellow/magenta/cyan (their addition leads to

black). In pigments (subtractive chemical systems), it can be distinguished multiple causes (phenomena) leading to absorption bands but actually, it can be considered only three main kinds of spectral signature. For illustration, this could be schematized considering co-doped Co^{2+}/Ga^{3+}-ZnO, as shown in Figure 1. This example is chosen because the three main kinds of spectral signatures all occur; it does not mean the work proposed in this article is limited to doped-inorganic oxides with semiconducting properties. In zinc oxide, well-known as one of the most effective UV shielding agents [20,21], the semi-conducting properties are coming from the band gap of about 3 eV (at the frontier between UV and visible ranges) separating the valence band (VB: issued from the "anionic atomic orbitals") and the conductive band (CB: issued from the "cationic metal orbitals") (Figure 1a). Thus, the UV light is with enough energy to promote electrons transfer from VB to CB and is absorbed. The spectral signature is a sigmoid curve quickly decreasing from a near total absorption in UV to a near total reflection in visible range. The doping with a cationic chromophore ($3d^7$ electronic configuration Co^{2+} ion) inserted into a tetrahedral crystal field (Figure 1b) leads to a visible absorption (Gaussian envelop) in the orange region. Taking for treatment the d^3 Tanabe-Sugano (TS) diagram for octahedral field: equivalent to d^7 TS diagram in tetrahedral field (as well known, d^n TS diagram in tetrahedral field are equivalent to d^{10-n} diagram in octahedral field), it corresponds to the $^4A_2$ fundamental state up to the $^4T_1$ second excited state transition) [22,23]. Thirdly (Figure 1c), the aliovalent doping with Ga^{3+} is supported by the creation of free electrons (for electroneutrality conservation) into the CB. The free electron gas, which can be described using Drude theory [24], acts as a barrier for radiation frequencies below plasmon frequency. Then a reverse sigmoid curve (with respect to the band gap sigmoid) is obtained with absorption of all low energy wavelengths, typically with a position at the frontier in between infrared and visible ranges.

In general, the skills of researchers working on the elaboration of new pigments can be quickly sum-up as moving in a predictable way these three signature positions: (i) band gap tuning, which is achieved mainly acting on the ionic/covalent balance of the metal-ligand bonds, (ii) Gaussian position which can be tuned taking into account the crystal field splitting (coordination and geometry of the interstitial sites) and or crystal field intensity (also depending on the ionic/covalent balance of the metal – ligand bonds), (iii) the plasmon frequency,

which is firstly depending on the free carriers concentration into the CB. These different manipulations are already well referenced, for illustration, on doped ZnO pigments [25].

As the aim of the article is not to enable the construction of pigments associated with desired spectra, whose color would be calculated by the methods proposed here. On the contrary, with this latter example, it can be shown that a single material can present a very complex spectrum with different types of absorption bands: for example, Co^{2+}/Ga^{3+}-ZnO is combining absorption bands of intra-atomic, inter-atomic and plasmonic origin, that would be more than pretentious to predict "*ab-initio*" its spectrum from a chemical composition. Indeed, in archetypal fashion, the pigment combines three major types of electronic transfer, from the most local (intra-atomic electron transition on the 3d orbitals of the chromophore cobalt ion), through the interatomic transition between oxygen anions and zinc +II cations, and finally toward to the most complex: plasmonic effect due to the free electrons (in the conductive band of such semiconducting oxide) due to the n-type doping (Ga^{3+}-Zn^{2+} substitution).

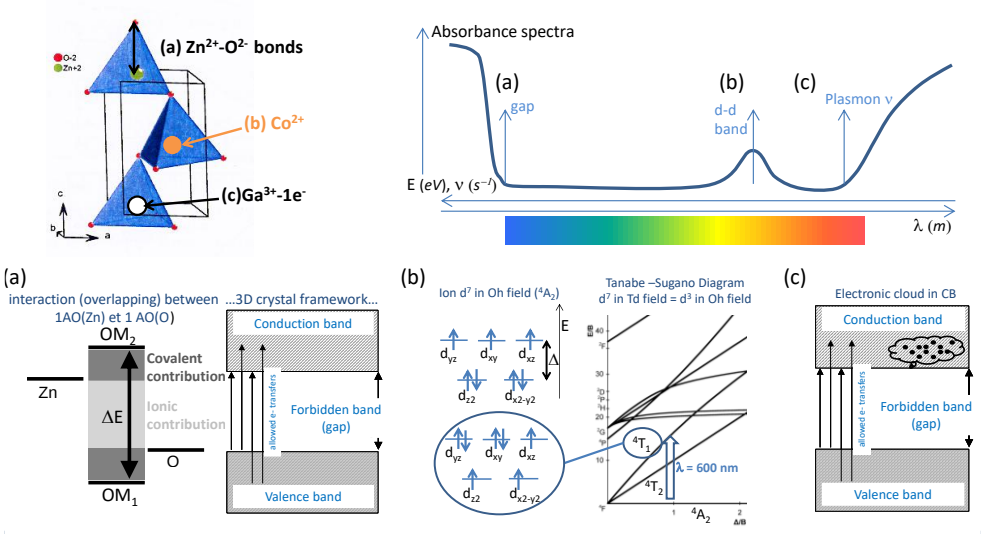

Figure 1: On a single oxide (Ga-Co co-doped ZnO), the three kind of electronic transfers responsible from the three kinds of absorption signatures: (a) inter-atomic e^- transfers: BV→ BC transfers (high-to-low sigmoid), (b) intra-atomic e^- transfers: Co^{2+} d-d transitions (Gaussian band), (c) delocalized electron gas: plasmon effect (low-to-high sigmoid).

2.2. Color modelling methodology

The Gaussian bands are created with a use of Excel spreadsheet or equivalent. It has been considered that the materials are 100% white out of the regions impacted

by the Gaussian absorbed bands. Thus, a spectrum can be created just depending on the number of Gaussian bands we created, with three parameters for each Gaussian can to consider: the width, the intensity and the position (in energy/wavelength) of the band. To each spectrum it can be associated a color. We have used to calculate the color associated with each spectrum, the x (λ), y(λ) and z(λ) trichromatic functions which are defined by the CIE with the 1964 illuminant, based on a 10° stimulus. The colors are then expressed in L*, a*, b* trichromatic system which is largely the most commonly used trichromatic space in pigment industry.

The Gaussian's position, intensity and width parameters could then be adjusted to minimize the color deviation of a calculated color besides a color target. It has to be understood that the work is not only a fit but the creation (by a least-square methods) of spectra in order to match a target color. This deviation between the calculated color (CC) associated to the created spectra (with L^*_{CC}, a^*_{CC} and b^*_{CC} parameters) and the target colors (with L^*_{TC}, a^*_{TC} and b^*_{TC} parameters), is treated by the minimization thanks to excel solver of the optical contrast, ΔE such as:

$$\Delta E = [(L^*_{CC}-L^*_{TC})^2 + (a^*_{CC}-a^*_{TC})^2 + (b^*_{CC}-b^*_{TC})^2]^{0.5}.$$

Intensity, position and width of the Gaussian bands are let to be adjusted during the ΔE minimizing iterations. Excel solver was used to minimize the ΔE.

As the Gaussian shapes for absorption bands are obtained in energy axis not in wavelength axis, all the spectra in the article are exhibited versus energy (eV).

2.3. Colors associated with a single phenomenon

As an introduction of the modelling operations proposed in the article, we looked for the literature for accessible color models with a single phenomenon (sigmoid 1, sigmoid 2 or Gaussian) without success. Only basic models are available, such as the presentation of the color scale from white to black, passing through yellows and then reds for semiconductor colors [1-2]. A sigmoid has four variable settings: slope sharpness, maximum absorption intensity: upper plateau, minimum absorption intensity: bottom plateau and inflection point position. Similarly, a Gaussian has four variable settings: width, maximum absorption (height of the curve's peak), minimum absorption (background noise), and position. Here, we illustrate for sigmoids of fixed sharpness, fixed absorption intensities (from 0 to 100 in the Kubelka-Munk absorbance scale: K/S) and variable positions, and in the

same way for Gaussian: fixed width and absorption (from 0 to 100) and variable positions. It can be noted that sigmoid and Gaussian curves are defined in absorbance space (K/S coordinates), but that we make the choice to depict diffuse reflection spectra, thanks to the basic relation: $K/S = (1-R)^2/2R$ [26]. All modelled spectra can easily lead to the colorimetric parameter calculation using the x, y z, trichromatic functions as defined by the CIE (International Commission of Illumination [27]). Then, pathway matrix was used to transform x, y z as-obtained coordinates in L, a*, b* colorimetric space, which is commonly used in pigments and dyes field [28]. Colors associated to each Gaussian or sigmoids positions, for the three kinds of phenomena which can be encountered in solid state pigments, are illustrated in Figure 2. We can observe that a limited color scale is reached for the two sigmoidal signatures (from pale yellow to deep red for band-gap semi-conductors and from deep blue to light cyan for plasmon gas).

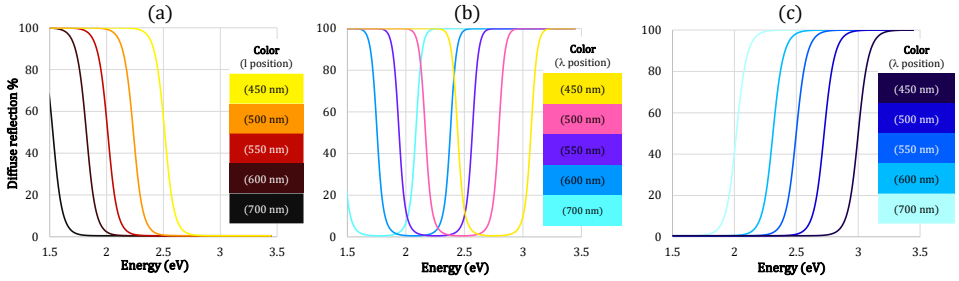

Figure 2: The archetypical colorations which are accessible for pigments with only one of the three kinds of absorption signatures: (a) high-to-low sigmoid, (b) Gaussian band, (c) low-to-high sigmoid.

With the aim of simplifying more complex modelling and helping chemists choose chemical substitutions or doping to improve pigment colors, it appears that the addition of sigmoidal curves is clearly not necessary. Indeed, it can be shown that a sigmoid can be fitted by a half-Gaussian (or similarly, a Gaussian of large width whose central position is outside the visible range). As shown by the sigmoid tests with different degrees of sharpness (with shallow slopes at the inflexion point), the colorimetric parameters derived from sigmoids or half-Gaussian best-fit sigmoids are very close (Figure 3). They are very similar for sigmoids with shallow slopes, and slightly different for sigmoids with smooth slopes. The fit of the Gaussians to the sigmoids was carried out using a method that will be repeated throughout this article: with a use of Excel spreadsheet or equivalent, the Gaussian's position and width parameters were adjusted to minimize the color deviation, also known as

optical contrast, ΔE between the colorimetric parameters obtained with the sigmoid and the Gaussian curves: $\Delta E = [(L_G-L_S)^2 + (a_G^*-a_S^*)^2 + (b_G^*G-b_S^*)^2]^{0.5}$.

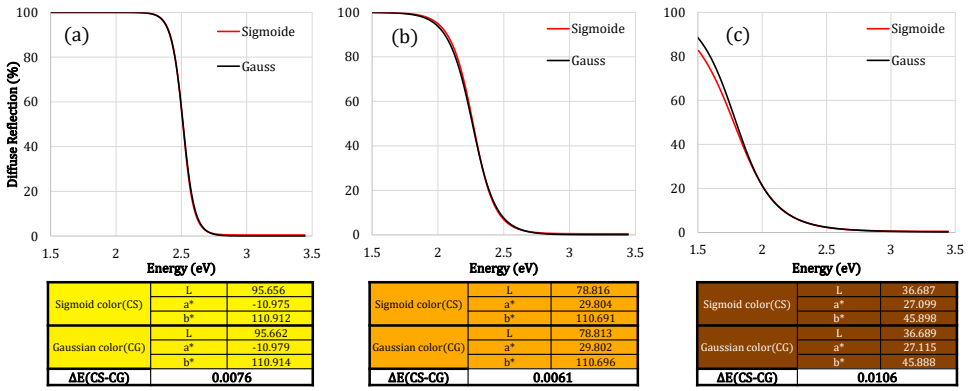

Sigmoid color(CS)	L	95.656
	a*	-10.975
	b*	110.912
Gaussian color(CG)	L	95.662
	a*	-10.979
	b*	110.914
ΔE(CS-CG)	0.0076	

Sigmoid color(CS)	L	78.816
	a*	29.804
	b*	110.691
Gaussian color(CG)	L	78.813
	a*	29.802
	b*	110.696
ΔE(CS-CG)	0.0061	

Sigmoid color(CS)	L	36.687
	a*	27.099
	b*	45.898
Gaussian color(CG)	L	36.689
	a*	27.115
	b*	45.888
ΔE(CS-CG)	0.0106	

*Figure 3: Comparison of the La*b* colours obtained from a high-to-low sigmoid and a Gaussian half curve fitting the sigmoid for (a) a sharp signature to (c) a smooth signature.*

2.4. Colors associated with a single phenomenon

Thanks to our ability to easily simulate an optical spectrum as a linear combination of Gaussians (in K/S absorption space) and then obtain equivalent diffuse reflection spectra, the proposal of diffuse reflection spectra associated with each of the 6 "primary" colors (Red, Green Blue and Cyan, Magenta, Yellow) was considered. First of all, these colors are combined with the best possible solutions in the simplest spectral space conceivable: spectra comprising a single intense absorbance phenomenon (a single Gaussian of maximum intensity fixed at saturation: K/S = 100 set against a continuous background of zero: none other absorbance). Only the width and the position of the single Gaussian absorption band were left free to be adjusted to target the six series of La*b* parameters corresponding to the six primary colors. The plots of the reflectance spectra with targeted La*b* and calculated La*b* are reported in Figure 4.

A perfect magenta was obtained with an absorption band centred in the green part of the spectrum, just in the middle of the visible range (the ΔE optical contrast error obtained by difference between theoretical and calculated magenta are equals to 1.10^{-3}). This very good result is without any doubt obtained thanks to the maximal sensitivity of human vision on the green part of the light spectrum, green being the just complementary color of magenta. In opposite way, no wavelength range is associated with magenta coloring and consequently it is not possible to propose a

single-Gaussian reflection spectrum that can be associated with green coloring. Average quality fits are achieved for blue, yellow, cyan. For red colors, a poor matching is reached. The distribution of the eye sensitivity for the reddish component in the two extreme parts of the spectrum (low wavelengths below 450 nm and high wavelengths beyond 600 nm) combined with a poor sensitivity of human vision in these two regions may explain the most important difficulty to achieve a red coloration with a single-Gaussian spectrum.

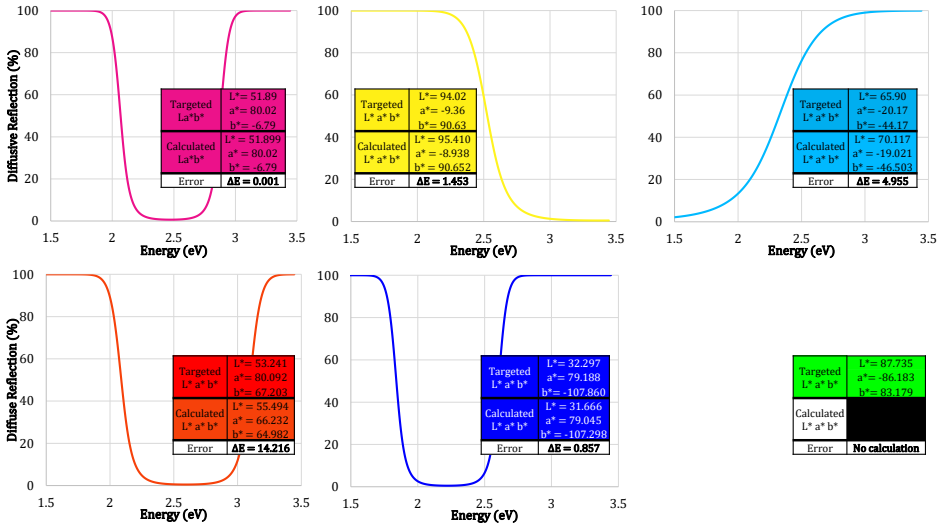

Figure 4: The best single Gaussian signals targeting the 6 main colours (Cyan, Magenta, Yellow, Red, Blue and Green).

To pursue this idea, a new series of spectra with, this time, two Gaussian absorption phenomena (still with intensities fixed at K/S =100 and on a non-absorbing background) were proposed in order to try to obtain the six primary colors. The results are shown in Figure 5. With the combination of two Gaussians, all six primary colors can be well fitted. However, the green and especially the red color remain (ΔE about 5) with a truly significant optical contrast between calculated and target color. Nonetheless, ΔE contrast equal to about 4 (depending the authors) is considered to be the critical value enabling the human eye to distinguish between two colors [30-32]; it can be therefore be said that the six primary colors are indeed characterized by two-Gaussian spectra.

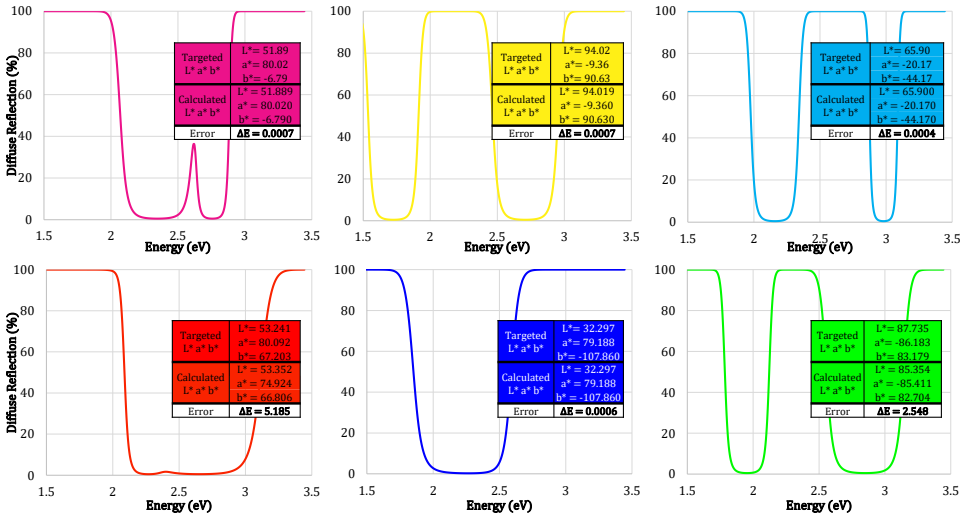

Figure 5: Some double Gaussian signals targeting the 6 main colours (Cyan, Magenta, Yellow, Red, Blue and Green).

2.5. A surjective transformation from color to spectra and some consequences

Actually, while a double Gaussian spectrum whose two Gaussian positions and width are left free to be adjusted for reaching a target color, different solutions with almost identical correlation factor values can be found. These different solutions can be obtained when the starting Gaussian positions and widths before adjustments are chosen with drastically different values. Two-Gaussian spectra constitute school-example of the surjection operating from color space to spectra space. Illustrations of various spectra that can be proposed to correspond to a cyan and a yellow coloration are reported in Figure 6. Notably, it is interesting to note that the last two cyan spectra reported in Figure 6 seem quite opposite while given colors are similar.

In the field of the chemistry of pigments or dyes, routine research and development work often carried out consists, starting from a compound with interesting colorimetric parameters, in carrying out slight chemical modifications (by doping typically) in order to shift the energy of the absorption phenomena and thus obtain a wider range of accessible colorations. Many examples of research works consisting in accurately studying a solid solution varying a chromophore concentration into a matrix can be cited in this way (it could be cited the recent review of Pfaff as a case in point [33]. Also, with roughly the same approach, the development of chromogenic pigments (pigments able to change their coloration *versus* an external stimulus [34-36]) has been receiving growing attention during

these last decades. These pigments are developed for their sensing applications, as thermochromic pigments can be employed in order to mark a thermal history [37-40] or piezochromic pigments can be used to detect shocks [12-13,41-43]. Good chromogenic pigments are the ones with a large change of their coloration *versus* the external stimulus. Thus, a good way to propose optimized chromogenic pigments is to focus on pigments with adequate diffuse reflection spectra, whose corresponding color is very sensitive to slight energy shift of the absorption bands. It can be noted, that *a contrario*, robust pigments with color stable despite some possible pollutions or environmental variation can be also required. So, this very important property for a pigment to be drastically tuned, or on the contrary not, from a modification of the absorption band energy is a fundamental aspect to consider for pigments and dyes production. Empirical approach seems always dominating. However, a first questioning of the possibilities of color variation from a spectrum obtained seems crucial.

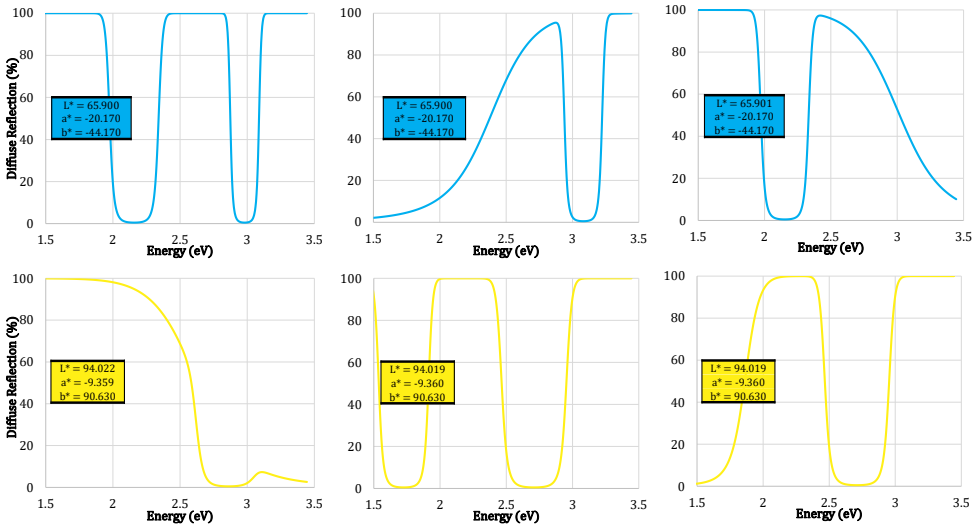

Figure 6: Various double Gaussian signals targeting the Cyan and Yellow with same result qualities.

From our calculated spectra, it is interesting to observe that from a same color but from different spectra (associated to different compounds), the same energy shift can lead to different color variation results as shown in Figure 7 for yellow color, and in Figure 8 for cyan color. Here, into a first approximation, the choice was made to "simulate" a chemical doping impact by shifting the two absorbance bands in the same direction (moving both the bands toward lower energy: -0.1 eV was applied, or both the bands toward higher energy: +0.1 eV was applied). Obviously,

depending on the origin of the absorption phenomena, opposite energetic displacements can be observed: typically increasing the covalency of metal-ligand bonds can increase not only the band-gap but also the Racah parameter, leading to a shift toward low-energy in intra-atomic electron transitions. It can be also note that d-d intra-atomic transitions can be can be proportional to the crystal field, doubly proportional to the crystal field, or even inversely proportional to the crystal field (as respectively for the $^4T_1 \rightarrow {}^4T_2$, $^4T_1 \rightarrow {}^4A_2$, $^4T_1 \rightarrow {}^2E$, three first transitions of the d^7 configuration TS diagram).

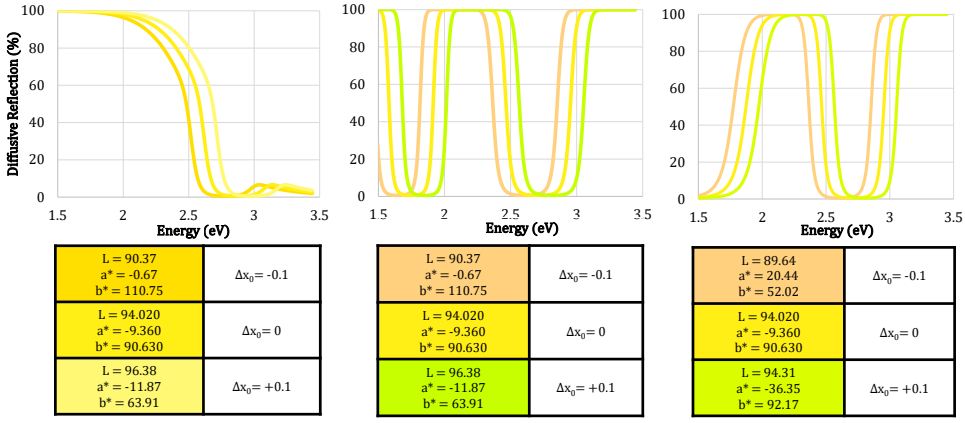

Figure 7: Sensitivity of different the "yellow" double Gaussian signals to an energy shift of the absorbance phenomena.

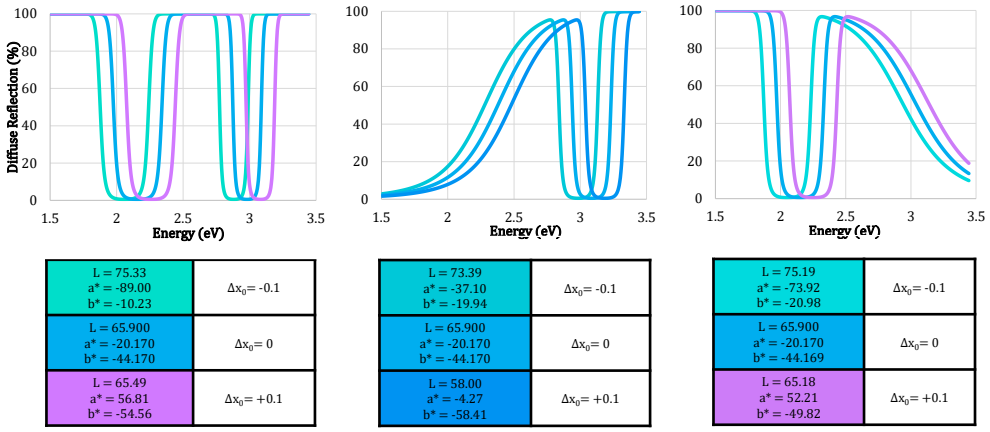

Figure 8: Sensitivity of different the "Cyan" double Gaussian signals to a Δx_0 energy shift (in eV) of the absorbance phenomena.

Clearly, for both yellow and cyan colors, some spectra lead to a color robustness versus band shift: the first yellow spectrum, the second cyan spectrum) whereas other spectra are really sensitive to absorption shifts: with a change from a green coloration (energy shift Δx_0 = -0.1 eV) to pink salmon coloration (Δx_0 = +0.1 eV) for the second yellow spectrum, for instance.

We learned that a color is not associated with a robust or mutable behaviour besides chemical modification and/or temperature effect. Regarding the controversy surrounding the origin of the drastic temperature-dependent color change in Cr-doped Al_2O_3 [44-47] (ruby solid solution with temperature-dependent change from pink to green), based on our calculations, it can be clearly stated that this notable thermochromism stems from the shape of the diffuse reflection spectrum (with two sharp bands associated with the two visible d-d transitions of the chromophore cation Cr^{3+} ($3d^3$ electronic configuration) and not from the special colorimetric situation of pink and green coloration (complementary colors) as is sometimes proposed in the literature. Further tests, using triple or quadruple Gaussian signals tend to show that spectra made up of multiple narrow transitions offer greater versatility than absorption band energy shifts.

Last part is devoted to metamerism: dependency of the perception of a color versus spectral power distribution, namely the illuminant. The different double-Gaussian signals leading to a single yellow or cyan color were also used to study the robustness/versatility of the color perceived under irradiation with various illuminants (taking blackbody radiation corresponding to various temperatures : 3000, 65000 and 10000 K, corresponding to the twilight, standard daylight and zenithal summer illumination). For this last series of models, due to the mandatory normalization of the maximum intensity of the illuminant (at 100%), the luminosity parameter (L) becomes physically meaningless. Consequently, only the chromatic parameters a* and b* need to be examined. The spectra obtained under different illuminants are plotted in Figure 9 for the yellow plots and Figure 10 for the cyan plots.

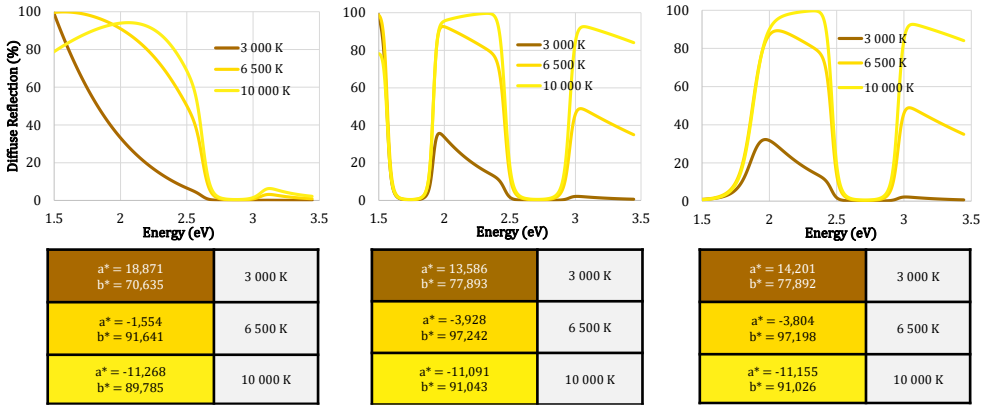

Figure 9: Sensitivity of different the "yellow" double Gaussian signals to the illuminant spectra (taken as pure black body radiation with various Wien temperatures)

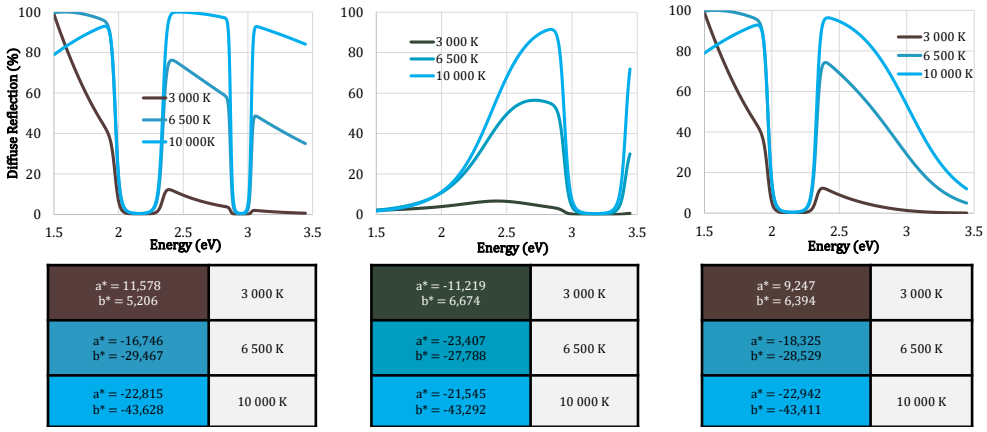

Figure 10: Sensitivity of different the "cyan" double Gaussian signals to the illuminant spectra (taken as pure black body radiation with various Wien temperatures)

The first point to note is that cyan color can be sensitive in different ways to the decrease of the illuminant temperature depending on its associated spectrum: in one case it turns into a dark greenish coloration (a*: green –red chromatic axis, with a negative value), and in the two other cases, into a reddish-brown coloration (a* with positive value). Without juxtaposition with another color that is less sensitive to the illuminant temperature and can serve as reference, it is therefore impossible, even for the complex human brain, to have any chance of correcting the distorted cyan coloration induced by low temperature illuminants (and therefore with a non-negligible reddish "background") using a white balance. Clearly, the white color,

associated with no absorption phenomenon in the visible range, evolves in a unique way as a function of the illuminant, and can always be used by the human brain to process the panel of colors perceived in a colored landscape, in order to rectify chromatic distortions caused by illuminant instabilities. Our experiments tend to show that the color light yellow also appears to be a robust color in relation to the illuminant (low metamerism). Despite the construction of three very different spectra to establish the single yellow color, the metamerism of the three spectra is very similar, i.e. with the same tendency to evolve slowly from yellow to orange to brown as the temperature of the illuminant decreases.

3. Conclusion

Firstly, it has been reminded that pigments (whatever their composition, or their insulating or semiconducting properties) exhibit three absorbance signature positions: (i) band gap due to interatomic transfers, (ii) Gaussian absorption band form intra-atomic transfers within chromophore cation's orbitals, (iii) the plasmon absorbance beyond the plasma frequency, which is firstly depending on the free carriers' concentration into the CB. Even if band gap and plasmon phenomena are associated with sigmoidal curves, it was shown that each of the three main signatures can be approximated using only Gaussian functions. Hence, diffuse reflectance spectra were created to fit as the best the 6 main colors: Red/Green/Blue and Cyan/Magenta/Yellow, firstly considering spectra with a single Gaussian absorption phenomenon and then, in a second time, considering spectra with two Gaussian absorption phenomena. The six primary colors are shown to be very well created from two-Gaussian spectra. In this first work step, the proposed process (easy to implement from a basic spreadsheet) to create various spectra can be used to help the pigments creator to optimize pigments composition in order to produce the energy shift of the absorbance bands (from crystal filed or iono-covalency balance modification) is the good direction for achieving the target coloration. Obviously, since several chemical principles can alter the position, width and intensity of absorption bands in different ways, it could appear a trcky issue to predict the evolution of these absorption band parameters. However, our proposal is no less useful, as the experimenter making pigment cannot avoid to manipulate this complex framework. When the experimenter obtains an orange pigment when he wanted it to be red, he has already to act chemically (on the compound

composition) to produce the displacement, widening or variation in intensity of the absorption bands involved. Typically, the chromophore concentration, the iono-covalence of the bonds to vary the crystalline field or the gap, the introduction of a second chromophore to introduce new corrective absorption bands, etc., can all be manipulated. This is precisely what our model is all about with the proposition that before moving on to the experiment (compound modification), our model will enable him to see much more clearly the spectral modifications to be made to achieve the desired color (the red pigment) from what he has previously obtained (the orange pigment).

Also, interestingly, as it is well known, different spectra can lead to a same color and the two-Gaussian spectra constitute school-example of the surjection operating from color space to spectra space. This behaviour can be exploited to create more robust (or more mutable) coloration versus external modification acting on color (as the illuminant: metamerism or as the temperature: thermochromism, for illustration). Indeed, the development of chromogenic pigments mutable color pigments able to change significantly their coloration *versus* an external stimulus has been receiving growing attention during these last decades for their sensing applications. We have shown that, associated to a perfectly same color, some different spectra lead to a color robustness whereas other spectra are sensitive to absorption shifts. On the other hand, some colors (yellow) seem inherently less prone to strong metamerism than others (cyan). The fundamental work proposed would constitute an important brick for who wants to develop new pigments basing on spectral strategies for the elaboration of efficient color control.

Funding. This study was carried out with financial support of the "agence nationale de la recherche", ANR DEFINED (ANR-20-CE09-0032).

Disclosures. The authors declare no conflict of interest.

Data availability. Data supporting the results presented in this paper can be obtained from the authors upon reasonable request.

References

1. Nassau K, The Physics and Chemistry of Color: The fifteen causes of color, New York (USA): John Wiley & Sons; 1983.
2. Tiley RJD, Colour and the optical properties of materials: An exploration of the relationship between light, the optical properties of materials and colour. New York: John Wiley & Sons; 2010.
3. Brittish Library, Science Blog 2017.
https://blogs.bl.uk/science/2017/07/william-perkin-and-mauveine.html
4. LibQuotes, Leigh Hunt quote from the Seer, 1964.
https://libquotes.com/leigh-hunt/quote/lbt4w8r
5. Gizmodo, Menegus B. The difference between RGB and CMYK, explained, 2016.
https://gizmodo.com/the-difference-between-rgb-and-cmyk-explained-1777830600
6. Bourkabi N, Theory of sets, Paris: Hermann; 1986.
https://en.wikipedia.org/wiki/Surjective_function
7. Crosby PHN, Netravali AN. Green Thermochromic Materials: A Brief Review. Adv Sustain Sys 2022;6:2200208,
8. Hakami A, Srinivasan SS, Biswas PK, Krishnegowda A, Wallen SL, Stefanakos EK. Review on thermochromic materials: development, characterization, and applications. J Coat Technol Res 2002;19:377–402.
10. Gaudon M, Carbonera C, Thiry AE, Demourgues A, Deniard P., Payen C, Létard J-F, Jobic S. Adaptable thermochromism in the $CuMo_{1-x}W_xO_4$ series ($0 \leq x < 0.1$): A behavior related to a first-order phase transition with a transition temperature depending on x. Inorg Chem 2007;46:10200–10207.
11. Guan S, Souquet-Basiège M, Toulemonde O, Denux D, Penin N, Gaudon M, Rougier A. Toward room-temperature thermochromism of VO_2 by Nb doping: magnetic investigations. Chem Mater 2019;31:9819–9830.
12. Righetti L, Robertson L, Largeteau A, Vignoles G, Demourgues A, Gaudon M. $Co_{1-x}Mg_xMoO_4$ compounds for pressure indicators. ACS Appl Mater Interfaces 2011;3:1319–1324
13. Blanco-Gutierrez V, Demourgues A, Lebreau, E, Gaudon M. Phase transitions in $Mn(Mo_{1-x}W_x)O_4$ oxides under the effect of high pressure and temperature. Phys Status Solidi B, 2016;253:2043–2048.
14. Blanco-Gutierrez V, Cornu L, Demourgues A, Gaudon M. $CoMoO_4/CuMo_{0.9}W_{0.1}O_4$ mixture as an efficient piezochromic sensor to detect temperature/pressure shock parameters. ACS Appl Mater Interfaces 2015;7:7112–7117.
15. Burns SA, Chromatic adaptation transform by spectral reconstruction. Color Res Appl 2019;44:682-693
16. Shi K, Luo MR. Factors affecting colour matching between displays. Opt Express 2022;30:26841–26855.
17. Derhak MW, Roy LL, Berns S. Wpt (waypoint) shift manifold difference metrics for evaluation of varying observing-condition (observer + illuminant) metamerism and color inconstancy. Color Res Appl 2020;45:1005-1022
18. Xu J, Luo MR, Fan H. Testing methods to estimate spectral reflectance using datasets under different illuminants. Color Res Appl 2023;48:368–380.
19. Valeur B, La couleur dans tous ses éclats. Paris : Belin, 2011.
20. Silva MRF, Alves MRFP, Cunha JPGQ, Costa JL, Silva CA, Fernandes MHV, Vilarinho PM, Ferreira P. Nanostructured transparent solutions for UV-

shielding: Recent developments and future challenges. Mater Today Phys 2023;35:101131.
21. Parwaiz S, Khan MM, Pradhan D. CeO_2-based nanocomposites: An advanced alternative to TiO_2 and ZnO in sunscreens. Mater Express, 2019;9:185–202.
22. Gaudon M, Toulemonde O, Demourgues A. Green coloration of co-doped ZnO explained from structural refinement and bond Considerations. Inorg Chem 2007;46:10996–11002.
23. Mjejri, Mornet S, Gaudon, M. From nano-structured polycrystalline spheres with $Zn_{1-x}Co_xO$ composition to core-shell $Zn_{1-x}Co_xO@SiO_2$ as green pigments. J Alloys Compd 2019;777:1204–1210.
24. Drude P. Zur Elektronentheorie der Metallen. Annalen der Physik. 1900;306:566–613.
25. Serier H, Demourgues A, Gaudon M. Investigation of Ga substitution in ZnO powder and opto-electronic properties. Inorg Chem 2010;49:6853–6858.
26. Kubelka P, Munk F. Ein Beitrag zur Optik der Farbanstriche. In: Zeitschrift für technische Physik. 1931;12:593–601.
27. CIE, International commission on illumination /Commission Internationale de l'Eclairage. Official website. http://cie.co.at/index_ie.html
29. CIELAB color space. Wikipedia, the free encyclopedia. https://en.wikipedia.org/wiki/CIELAB_color_space
30. Witzel RF, Burnham RW, Onley JW. Threshold and suprathreshold perceptual color differences. J Opt Soc Am, 1973;63:615-625.
31. Wright WD. A re-determination of the trichromatic coeffients of the spectral colours. Trans Opt Soc, 1929;30:141-164.
32. Wyszecki G, Fielder GH. New color-matching ellipses. J Opt Soc Am, 1971;61:1135-1152.
33. Pfaff G. Mixed metal oxide pigments. Phys Sc Rev 2022;7:7–16.
34. Granqvist CG, Green S, Niklasson GA, Mlyuka NR, von Kræmer S, Georén P. Thin Solid Films 2010;518:3046-3053
35. Granqvist CG, Lansåker PC, Mlyuka NR, Niklasson GA, Avendaño E. Progress in chromogenics: New results for electrochromic and thermochromic materials and devices. Sol Energy Mater Sol Cells 2009;932032–2039.
36. Rossi S, Simeoni M, Quaranta A. Behavior of chromogenic pigments and influence of binder in organic smart coatings. Dyes Pigm 2011;184:108879.
37. Copin EB, Massol X, Amiel S, Sentenac T, Le Maoult Y, Lours P. Novel erbia-yttria co-doped zirconia fluorescent thermal history sensor. Smart Mater Struct 2017;26:015001.
38. Rabhiou A, Feist J, Kempf A, Skinner S, Heyes A. Phosphorescent thermal history sensors
Sens Actuators, A 2011;169:18–26.
39. Rabhiou A, Kempf A, Heyes A. Oxidation of divalent rare earth phosphors for thermal history sensing. Sens Actuators, B 2013;177:124–130.
40. González AY, Skinner S, Beyrau F, Heyes AL. Reusable Thermal History Sensing via Oxidation of a Divalent Rare Earth Ion-Based Phosphor Synthesized by the Sol-Gel Process. Heat Transfer Eng 2015;36:1275–1281.
41. Gaudon M, Thiry AE, Largeteau A, Deniard P, Jobic S, Majimel J, Demourgues A. Characterization of the piezochromic behavior of some members of the $CuMo_{1-x}W_xO_4$ series. Inorg Chem 2008;47:2404–2410.
42. Blanco-Gutierrez V, Demourgues A, Gaudon M. Sub-micrometric β-$CoMoO_4$ rods: Optical and piezochromic properties. Dalton Trans 2013;42:13622–13627.

43. Robertson L, Penin N, Blanco-Gutierrez V, Sheptyakov D, Demourgues A, Gaudon M. $CuMo_{0.9}W_{0.1}O_4$ phase transition with thermochromic, piezochromic, and thermosalient effects. J Mater Chem C 2015;3:2918–2924.
44. Nguyen DK, Bach Q-V, Kim B, Lee H, Kang C, Kim I-T. Synthesis of Cr-doped Al_2O_3 by Pechini sol-gel method and its application for reversible thermochromic sensors. Mater Chem Phys 2019; 223:708-714.
45. Sone K, Fukuda Y. Thermochromism of transition metal complexes in the solid state. Inorganic Thermochromism, Berlin/Heidelbreg (Germany), Springer, 1987:104-128.
46. Salek G, Devoti A, Lataste E, Demourgues A, Garcia A, Jubera V, Gaudon M. Optical properties versus temperature of Cr-doped γ- and α-Al_2O_3: irreversible thermal sensors application. J Lumin 2016;179:189-196.
47. Fahlman BD, Barron AR. CVD of chromium-doped alumina “ruby” thin films. Chem Vap Depos 2001;7:62-65.